CONF-880417--10

To be presented at the International Symposium on Fusion Nuclear Technology (ISFNT) to be held during the period of April 10-19, 1988, in Tokyo, Japan.

CONF-880417--10

DE88 009929

MHD THERMAL HYDRAULIC ANALYSIS OF THREE-DIMENSIONAL LIQUID METAL FLOWS IN FUSION BLANKET DUCTS*

by

T. A. Hua, B. F. Picologlou
C. B. Reed

Argonne National Laboratory
9700 S. Cass Ave.
Argonne, IL 60439

and

J. S. Walker
University of Illinois, Urbana, IL 61801

February 1988

*Work supported by the U. S. Department of Energy/Office of Fusion Energy under Contract W-31-109-Eng-38.

MHD THERMAL HYDRAULIC ANALYSIS OF THREE-DIMENSIONAL LIQUID METAL FLOWS IN FUSION BLANKET DUCTS*

T. Q. Hua, B. F. Picologlou, and C. B. Reed
Argonne National Laboratory, 9700 S. Cass Ave., Argonne, IL 60439 U.S.A.
J. S. Walker
University of Illinois, Urbana, IL 61801 U.S.A.

ABSTRACT

Magnetohydrodynamic flows of liquid metals in thin conducting ducts of various geometries in the presence of strong nonuniform transverse magnetic fields are examined. The interaction parameter and Hartmann number are assumed to be large, whereas the magnetic Reynolds number is assumed to be small. Under these assumptions, viscous and inertial effects are confined in very thin boundary layers adjacent to the walls. At walls parallel to the magnetic field lines, as at the side walls of a rectangular duct, the boundary layers (side layers) carry a significant fraction of the volumetric flow rate in the form of high velocity jets. The presence of these jets strongly enhances heat transfer performance. In addition, heat transfer can be further improved by guiding the flow toward a heated wall by proper variation of wall thicknesses, duct cross sectional dimensions and/or shape. Flows in nonconducting circular ducts are also examined. Experimental results obtained from the ALEX experiments at the Argonne National Laboratory are used to validate the numerical predictions.

*Work supported by the U. S. Department of Energy/Office of Fusion Energy under Contract W-31-109-Eng-38.

MHD THERMAL HYDRAULIC ANALYSIS OF THREE-DIMENSIONAL LIQUID METAL FLOWS IN FUSION BLANKET DUCTS

T. Q. Hua, B. F. Picologlou, and C. B. Reed
Argonne National Laboratory, 9700 S. Cass Ave., Argonne, IL 60439 U.S.A.
J. S. Walker
University of Illinois, Urbana, IL 61801 U.S.A.

1. INTRODUCTION

In a self-cooled liquid-metal blanket of a magnetically confined fusion reactor, the magnetohydrodynamic (MHD) effects are of paramount importance in the design process [1]. The interaction between the circulating liquid metal with the strong magnetic field necessary for confinement results in large electromagnetic body forces which determine the flow distribution of the liquid metal, and produce large MHD pressure gradients. The resulting MHD pressure drop may cause excessive pumping power loss and prohibitively large material stresses. Also, the MHD flow distribution may affect drastically the heat transfer characteristics of the blanket in general and the first wall coolant channels in particular. For these reasons, a predictive capability in MHD thermal hydraulics under reactor relevant geometries and conditions is an absolute necessity for the development of liquid-metal-cooled blankets and high heat flux devices. As a first step, capability for treating flows in single ducts has been pursued. Experience gained in this process will be used to treat multichannel complex geometries encountered in a fusion reactor.

This paper presents a summary of the computer codes developed jointly by Argonne National Laboratory (ANL) and the University of Illinois for the treatment of MHD flows in single ducts. The codes can treat ducts with thin conducting walls and circular, rectangular, or generalized cross section in a non-uniform transverse magnetic field. A circular duct with insulating walls in a non-uniform field has also been treated. The velocity distributions predicted by the MHD solutions are used as input to the energy equation and

the temperature distribution in the fluid is calculated in heat transfer modules which are part of the codes.

2. ANALYSIS FOR THIN CONDUCTING DUCTS

2.1 Governing Equations and Boundary Conditions

Consider the steady flow of an incompressible liquid metal driven by a pressure gradient along a conducting duct with thin metal walls and with an imposed transverse magnetic field whose strength varies along the duct. A transverse magnetic field variation in the axial direction requires a non-zero axial magnetic field. This weaker axial magnetic field is neglected in this model because the major electromagnetic body force in the liquid metal arises from the interaction between the fluid flow with the transverse field. The ratio of the induced to applied fields is given by $c^{1/2} R_m$. Here $c = \sigma_w t/\sigma L$ and $R_m = \mu\sigma U_o L$ are the wall conductance ratio and magnetic Reynolds number. μ and σ are the magnetic permeability and electrical conductivity of the liquid metal, σ_w and t are the electrical conductivity and thickness of the duct wall, U_o is the average axial velocity of the fluid and L is a characteristic transverse dimension of the duct. For a self-cooled blanket in a fusion device, $c^{1/2} R_m$ is at most of order 10^{-2}; therefore, it is appropriate to neglect the induced magnetic field.

The two important parameters in any general MHD problem are the interaction parameter, N, and Hartmann number, M, defined by

$$N = \frac{\sigma B_o^2 L}{\rho U_o} \quad \text{and} \quad M = L B_o \left(\frac{\sigma}{\rho \nu}\right)^{1/2}$$

where ρ and ν are the fluid's density and kinematic viscosity, and B_o, and U_o are the characteristic magnetic flux density and average velocity. In a fusion reactor, the values for M and N are typically of the order of 10^3 - 10^5 [1]. Under such conditions, inertial and viscous effects are confined in thin boundary and shear layers and are negligible in the core of the flow.

The inertialess, inviscid, dimensionless equations governing the flow of a liquid metal in the core of the flow are:

$$\nabla p = \underline{j} \times \underline{B}, \quad \underline{j} = -\nabla\phi + \underline{v} \times \underline{B}, \quad \nabla \cdot \underline{v} = 0, \quad \nabla \cdot \underline{j} = 0 . \qquad (1a,b,c,d)$$

Here p, $\underline{j}$, $\underline{v}$, and ϕ are the pressure, electric current density, velocity, and electric potential, normalized by $\sigma U_o B_o^2 L$, $\sigma U_o B_o$, U_o, and $U_o B_o L$, respectively. For $\underline{B} = B_y(x)\hat{y}$, the x, y, z core velocity components u_c, v_c, w_c, and electric current density components j_{xc}, j_{yc}, j_{zc}, which satisfy the equations (1) and the symmetry conditions, $j_y = v_c = 0$ at $y = 0$, are:

$$u_c(x,y,z) = \beta \frac{\partial \phi_c}{\partial z} - \beta^2 \frac{\partial p}{\partial x}, \quad w_c(x,y,z) = -\beta \frac{\partial \phi_c}{\partial x} - \beta^2 \frac{\partial p}{\partial z} \qquad (2a, 2b)\ (Cf.\ 1b)$$

$$v_c(x,y,z) = -y\beta'(x) \frac{\partial \phi_t}{\partial z} + y \frac{\partial}{\partial x}\left[\beta^2 \frac{\partial p}{\partial x}\right] + y\beta^2 \frac{\partial^2 p}{\partial z^2}$$

$$+ y \frac{\beta'^2}{2} \frac{\partial}{\partial z}\left[\left(r^2 - \frac{y^2}{3}\right) \frac{\partial p}{\partial z}\right] \qquad (2c)\ (Cf.\ 1c)$$

$$j_{xc}(x,y,z) = \beta \frac{\partial p}{\partial z}, \quad j_{zc}(x,y,z) = -\beta \frac{\partial p}{\partial x} \qquad (2d, 2e)\ (Cf.\ 1a)$$

$$j_{yc}(x,y,z) = -y\beta' \frac{\partial p}{\partial z} \qquad (2f),\ (Cf.\ 1d)$$

where $p(x,z)$ is the pressure which is constant along magnetic field lines by virtue of Eq. (1a), and $\beta(x) = B_y^{-1}(x)$. The electric potential in the core varies along the magnetic field lines according to

$$\phi_c(x,y,z) = \phi_t(x,z) - \frac{1}{2}(f^2 - y^2)\beta' \frac{\partial p}{\partial z} , \qquad (2g)$$

where $\phi_t(x,z)$ is the electric potential at the top wall which intersects the magnetic field line at $y = f(x,z)$. Equation (2g) is obtained by integrating the y- component of equation (1b), and using equation (2f).

The boundary conditions at the inside surface of a wall which has conductance ratio c_t and is not parallel to the magnetic field lines are

$$\underset{\sim}{v}_c \cdot \hat{n}_t = 0, \quad (\underset{\sim}{j}_c - \underset{\sim}{j}_w) \cdot \hat{n}_t = 0 \text{ at } y = f(x,z) \qquad (3a, 3b)$$

where $\hat{n}_t$ is a unit normal to the wall and $\underset{\sim}{j}_w = - c_t \underset{\sim}{\nabla}^2 \phi_t$. Conditions (3a, b) neglect the $O(M^{-1})$ jumps in $\underset{\sim}{v}_c$, $\underset{\sim}{j}_c$, and ϕ across the Hartmann layer, which has $O(M^{-1})$ thickness and separates the inviscid core region from the wall.

If a wall is parallel to the field lines (side wall), and has conductance ratio c_s, then the appropriate boundary condition is

$$(\underset{\sim}{j}_c - \underset{\sim}{j}_w) \cdot \hat{n}_s = 0 \qquad (3c)$$

here $\hat{n}_s$ is a unit normal to the side wall, and $\underset{\sim}{j}_w = - c_s \underset{\sim}{\nabla}^2 \phi_s$. Condition (3c) neglects $O(M^{-1/2})$ jump across the side wall layer which has $O(M^{-1/2})$ thickness. ϕ_s is the electric potential at the side.

The three-dimensional problem with eight variables in the core (p, ϕ, u_c, v_c, w_c, j_{xc}, j_{yc}, j_{zc}) is completely solved once the functions p,

ϕ_t, and ϕ_s are determined. The coupled partial differential equations (pde's) governing p, ϕ_t, and ϕ_s are derived by applying the boundary conditions (3a-3c). Special numerical schemes are developed to solve the pde's simultaneously.

2.2 Ducts with Circular Cross Section

For a straight circular duct duct, all lengths are normalized by the radius. The duct centerline is along the x- axis and the duct surface is given by $y = f(z) = \pm (1 - z^2)^{1/2}$. By virtue of symmetry, only one quadrant of the duct is considered, i.e. $0 \le z \le 1$, $0 \le y \le f(z)$.

The boundary conditions (3a, 3b) require that at $y = (1 - z^2)^{1/2}$.

$$(1 - z^2)^{1/2} v_c + z w_c = 0 \ , \ c \nabla^2 \phi_t = (1 - z^2)^{1/2} j_{yc} + z j_{zc} \qquad (4a,b)$$

Equations (4a) and (4b) constitute a pair of coupled pde's in $\phi_t(x,z)$ and $p(x,z)$ to be solved simultaneously by the finite difference method. Upstream (x_1) and downstream (x_2), where the magnetic field is uniform the flow is fully-developed. At $z = 1$ equations (4a,b) must satisfy the regularity conditions $(1 - z^2)^{1/2} \partial p/\partial z \to 0$ and $(1 - z^2)^{1/2} \partial \phi_t/\partial z \to 0$ [2]. Finally, at $z = 0$ the symmetry conditions $\partial p/\partial z = 0$, $\phi_t = 0$ apply.

Expansion and/or contraction of a duct with circular cross sections can easily be treated in a similar manner. The wall thickness can have an arbitrary variation in x and z provided symmetry about the $y = 0$ plane is preserved.

2.3 Ducts with Rectangular Cross Section

Consider a duct of variable rectangular cross section consisting of a straight portion, followed by a linear increase of the dimension which is parallel to the magnetic field lines, followed by another straight portion (Fig. 1a). The duct has a thin side wall, a thick side wall, and thin top and bottom walls of equal thicknesses. Such an arrangement with a series of expansions and contractions connected by straight rectangular ducts represents a judicious choice for the design of a blanket first wall coolant channel [3]. As a result of this arrangement, the flow is guided toward the thin side wall to improve heat transfer performance. The plane of symmetry being at y = 0, solution is sought over half the duct bounded by, $-1 \le z \le 1$, and $0 \le y \le f(x)$ where

$$f(x) = \begin{cases} a & \text{for} & x_1 \le x \le 0 \\ a + bx & \text{in expanding duct} & 0 \le x \le L_e \\ \hat{a} & \text{for} & L_e \le x \le x_2 \end{cases} .$$

The conductance ratios are c_t, c_1, and c_2 for the top wall, thin and thick side walls, respectively. The boundary conditions (3a,b) require that at y = f(x)

$$f' u_c - v_c = 0, \quad (1 + f'^2)^{-1/2}(f' J_{xc} - J_{yc}) = c_t\left[(1+f'^2)^{-1} \frac{\partial^2 \phi_t}{\partial x^2} + \frac{\partial^2 \phi_t}{\partial z^2}\right] \quad (5a,b)$$

and at $z = \pm 1$, condition (3c) gives

$$J_{zc}(x, -1) = c_1\left[\frac{\partial^2 \phi_1}{\partial x^2} + \frac{\partial^2 \phi_1}{\partial y^2}\right], \quad J_{zc}(x, +1) = -c_2\left[\frac{\partial^2 \phi_2}{\partial x^2} + \frac{\partial^2 \phi_2}{\partial y^2}\right] . \quad (5c,d)$$

Equations (5a,b,c,d) constitute four coupled pde's governing $p(x,z)$, $\phi_t(x,z)$, $\phi_1(x,y)$, and $\phi_2(x,y)$ which are solved simultaneously. At x_1 and x_2,

sufficiently far from the expansion, the flow is taken to be fully-developed; at y = 0 symmetry conditions are applied; at the corners z = ± 1 and y = f(x), electric potential and current must be continuous.

At z = - 1, (similar argument applies at z = 1), the transverse core current j_{zc} flows unchanged across the side layer and enters the side if $M^{-1/2} << c_1 << 1$ [4]. Some of the current entering the side flows up the wall (for y > 0), resulting in an O(1) electric potential in the side having a specific variation with y. Because the core potential at z = - 1 has a different variation with y, given by eq. (2g), there is a jump in the O(1) electric potential across the side layer, determining the O(1) volumetric flux in the side layer. The details of the side layer solution can be ignored provided that the total volumetric flux in the side layer plus the volumetric flux in the core is conserved at every cross section. By doing so a boundary condition for $\partial p/\partial z$ at z = - 1 can be derived [5]. The boundary conditions for eqs. (5a-d) are therefore completely defined.

2.4 Ducts with Arbitrary Cross Section

Consider an arbitrary cross section in Fig. 1b with the plane of symmetry at y = 0. The wall is divided into 6 segments denoted by letters "a" to "f". The pde's governing pressure and electric potential at segments "a", "c", "e", and "f" are derived by the methods described in Section 2.3. The governing equations for segment "d" is derived as follows. The coordinate at the wall is defined by $f(z) = a_o + \eta(z - z_d)$. The boundary conditions (3a,b) applied to this segment give:

$$\eta w_c - v_c = 0, \quad c\left[\frac{\partial^2 \phi_t}{\partial x^2} + (1 + \eta^2)^{-1} \frac{\partial^2 \phi_t}{\partial z^2}\right] = (1 + \eta^2)^{-1/2} (- j_{yc} + \eta j_{zc}) \quad (6a,b)$$

where w_c, v_c, j_{yc}, and j_{zc} are evaluated at $y = f(z)$. Continuity of electric potential and current density must be imposed at the junction between "c" and "d", and between "d" and "e".

Segment "b" is approximated by a series of small linear subsegments. The governing equations for p and ϕ_t are again given by Eqs. (6a,b) with n replaced by the slope of each subsegment.

3. ANALYSIS FOR A NONCONDUCTING CIRCULAR DUCT

The core equations are given by (1a, b, c, d) and (2a - 2g). In a nonconducting duct currents in the core must close through the Hartmann layer to complete the circuit. As a result, the $O(M^{-1})$ terms which are neglected in the case of a conducting duct, must be included in the asymptotic expansions, in order to determine the O(1) solution in the core. Each variable in the core or in the Hartmann layer, for instance p, is expanded in the form

$$p = p_o + M^{-1} p_1 + O(M^{-2}) \quad .$$

In the Hartmann layer, the normal components of velocity and current must vanish at the wall, and match their counterpart core variables at the core/Hartmann layer interface. Matching the O(1) terms gives boundary conditions for the core variables and the interfaces. Matching the $O(M^{-1})$ terms gives rise to two coupled pde's governing the O(1) pressure, $p_o(x,z)$, and O(1) electric potential, $\phi_o(x,z)$, at the inside surface of the duct.

4. THERMAL HYDRAULIC ANALYSIS

Once the velocity field is known from the MHD solution, the 3-D temperature profile in the fluid can be solved using the energy equation

$$Pe\left[u_c \frac{\partial T}{\partial x} + v_c \frac{\partial T}{\partial y} + w_c \frac{\partial T}{\partial z}\right] = \frac{\partial^2 T}{\partial x^2} + \frac{\partial^2 T}{\partial y^2} + \frac{\partial^2 T}{\partial z^2} \tag{8}$$

where T(x,y,z) is normalized by q"L/k; q" is the heat flux at the wall, L is the transverse characteristic length, k is the thermal conductivity and Pe is the Peclet number.

The boundary conditions necessary for the solution of Eq. (8) are well defined for most cases. If a heated wall has a side layer with significant mass flow rate, the boundary condition can be defined using either an explicit treatment or an integral treatment of the side layer. The explicit method employs an analytical solution for the side layer and a solution for the inviscid inertialess core. Since analytical solutions for the velocity profiles in the side layer exist only for uniform magnetic fields, this method is currently limited to flows in uniform magnetic fields.

The integral method uses the known mass flow rate in the side layer (given by the MHD solution) to calculate the fraction of heat flux convected in the side layer; the remaining heat flux is conducted into the core across the layer/core interface. This method approximates the average axial temperature gradient in the side layer by the axial temperature gradient at the interface. The integral method applies to flows in uniform and nonuniform magnetic fields. Although this method does not explicitly solve for the temperature distribution at the wall the maximum wall temperature occurs at the top and bottom of the side, where there is no flow in the side layer, and is nearly equal to the temperature at the interface.

5. RESULTS AND COMPARISON WITH EXPERIMENTS

An experimental facility, ALEX, has been built and is being operated at ANL to study liquid metal MHD phenomena relevant to fusion blanket engineering. Results for round and square test sections and comparison with numerical predictions have been reported [6]. Here, only a couple of representative results are given. Preliminary results of an ongoing test series involving flows through a rectangular duct with expansions and contractions are presented in a companion paper [3].

Figure 2 compares measurements with code predictions for the transverse pressure differences for the round duct, the pressure difference measured at z = 0 and z = 1. Figure 3 shows the axial velocity at y = 0 at the center of the duct (z = 0) and near the wall (z = 0.9) for the round duct. In fully developed flows, the pressure and axial velocity are uniform across z.

In uniform magnetic fields, the velocity can be guided toward one side wall by variation of duct cross sectional dimensions in a duct with unequal wall thicknesses. As an example, consider the geometry depicted in Fig. 1a. The conductance ratios are 0.014 for the top, bottom, and thin side walls, and 1.65 for the thick side wall. The top wall is at $y_t = 0.6$ for $x \leq 0$; $y_t = 0.6 + x/3$ for $0 \leq x \leq 2.4$; and $y_t = 1.4$ for $x \geq 2.4$. Figure 4 shows the evolution of the axial velocity as the liquid metal flows through the expansion. In addition to the desirable higher velocity distribution near the thin wall, the fraction of the total volumetric flow rate in the side layer also increases drastically (Fig. 5). Notice that the fraction of the flow in the side layer adjacent to the thick wall is negligibly small, because of the large conductance ratio there.

In a nonconducting circular duct, when the flow is fully developed, the velocity peaks at the center and vanishes near the wall. The non-uniformity

of the magnetic field causes the flow to migrate towards $z = \pm 1$, leaving a stagnant region in the center. Figure 6 shows such a development of the flow at Hartmann number of 10^4.

Figure 7 shows the fluid temperature distribution in a square duct at the midplane, $y = 0$, at three cross sections ($x = 0.3, 9.5, 17.5$). The side wall at $z = -1$ is heated uniformly from $x = 0$ to $x = 20$. The side layer carries 25% of the total flow rate. The Hartmann number (used to calculate the velocity in the side layer for the explicit method), the Peclet number, and the initial temperature are 10^4, 400 and 0.654, respectively. Results by the integral and explicit treatment of the side layer are compared. The slight differences in temperature at $z = -1$ indicate the small temperature drops across the side layer.

REFERENCES

[1] D. L. Smith, et al., "Blanket Comparison and Selection Study - Final Report," Argonne National Laboratory Report ANL/FPP 84-1 (1984).

[2] J. S. Walker and G. S. S. Ludford, "MHD Flow in Circular Expansions with Thin Conducting Walls," Int. J. Engrg. Sci. 13 (1975) 261-269.

[3] B. F. Picologlou, C. B. Reed, T. Q. Hua, J. S. Walker, L. Barleon and H. Kreuzinger, "MHD FLows Tailoring in First Wall Coolant Channels of Self-Cooled Blankets," Int. Symp. on Fusion Nuclear Technology, Tokyo (1988).

[4] J. S. Walker, "Magnetohydrodynamic Flows in Rectangular Ducts with Thin Conducting Walls, Part 1, Constant-Area and Variable-Area Ducts with Strong Uniform Magnetic Fields," J. de Mecanique Theorique et Appliquee, 20 (1981).

[5] T. Q. Hua, J. S. Walker, B. F. Picologlou and C. B. Reed, unpublished information (1988).

[6] C. B. Reed, B. F. Picologlou, T. Q. Hua and J. S. Walker, "ALEX Results - A Comparison of Measurements from a Round and a Rectangular Duct with 3-D Code Predictions," IEEE, 12th Symp. on Fusion Engrg. (1987).

LIST OF FIGURES

Fig. 1 Schematic of (a) a duct of variable ractangular cross sections, (b) an arbitrary cross section.

Fig. 2 Experimental data and code predictions for transverse pressure difference (12 o'clock - 3 o'clock) for a round duct which has a conductance ratio of 0.027. Also shown is the normalized magnetic field distribution.

Fig. 3 Experimental data and code predictions for the axial velocity at the midplane y = 0, at z = 0 (lower curve) and z = 0.9 (upper curve) for the round duct.

Fig. 4 Axial velocity profiles at the midplane y = 0, at various cross sections (See Fig. 1a for the geometry). The transverse magnetic field is uniform.

Fig. 5 Fraction of the total flow rate in the side layers adjacent to the thin wall (z = -1) and the thick wall (z = 1).

Fig. 6 Axial velocity profiles at the midplane y = 0 at various cross sections in a nonconducting round duct. The magnet field distribution is identical to that shown in Fig. 2.

Fig. 7 The temperature profiles in a square duct at the midplane y = 0 at three cross sections. Results by the integral method (solid lines) and the explicit method (dash lines) are compared. The heated wall is at z = -1, the other walls are adiabatic.

Figure 1 (Thanh Hua, et al.)

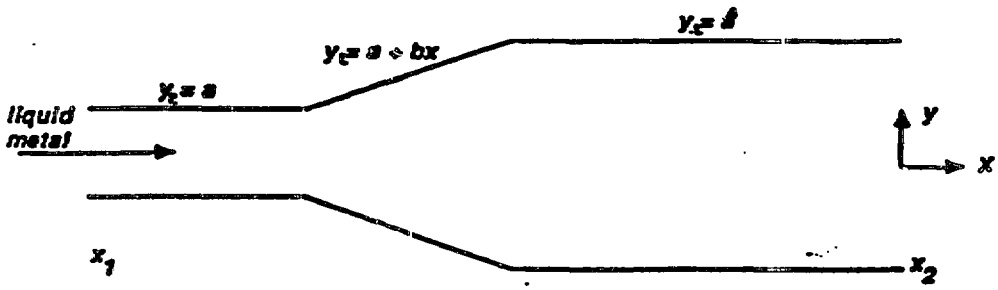

(a)

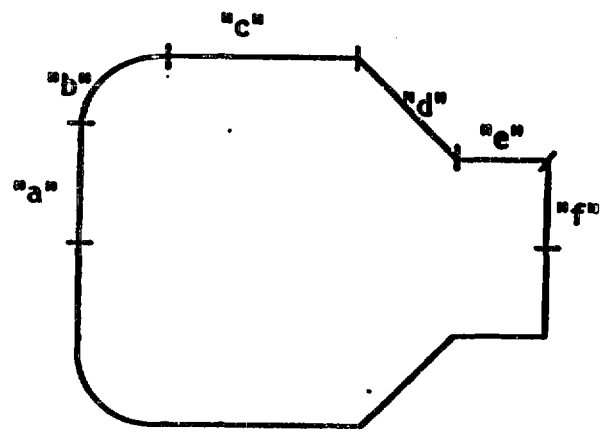

(b)

Figure 2 (Thanh Hua, et al.)

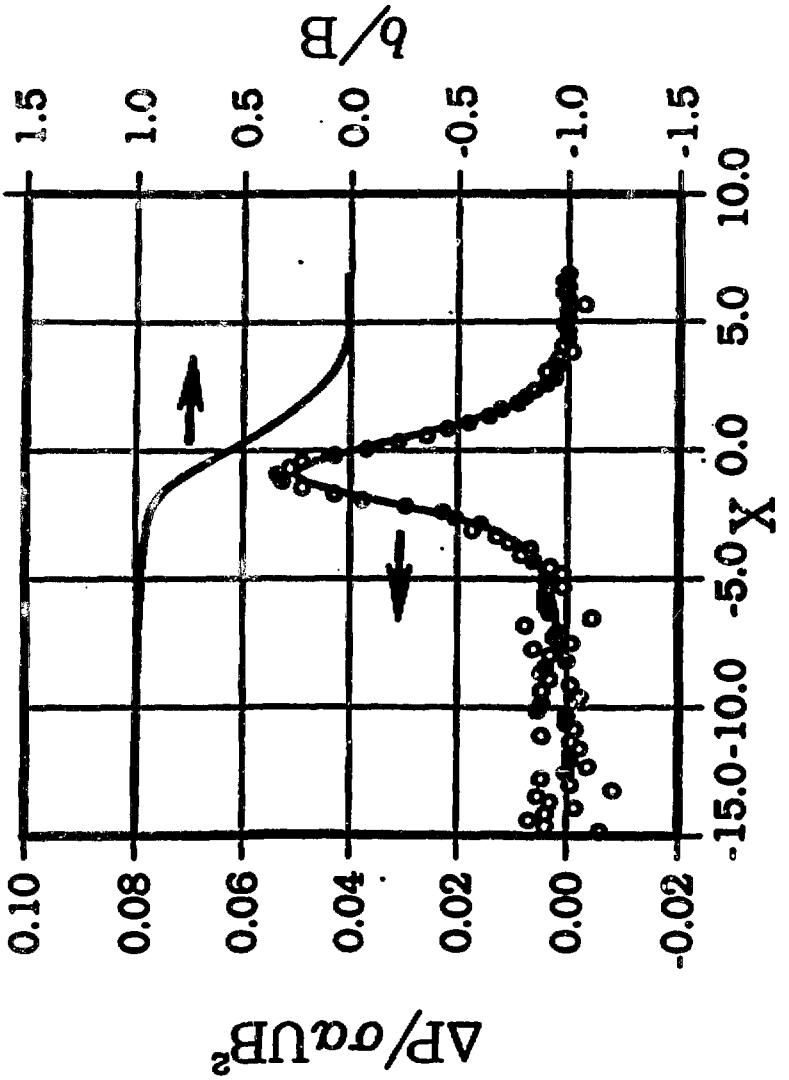

Figure 3 (Thanh Hua, et al.)

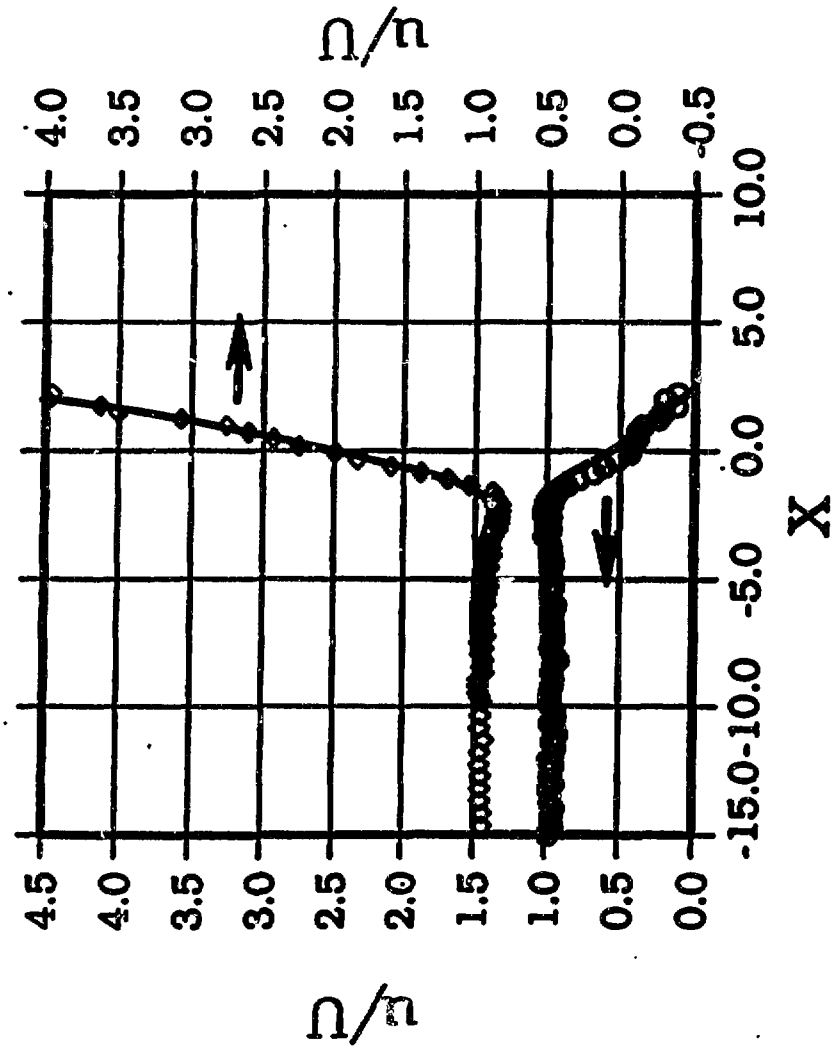

Figure 4 (Thanh Hua, et al.)

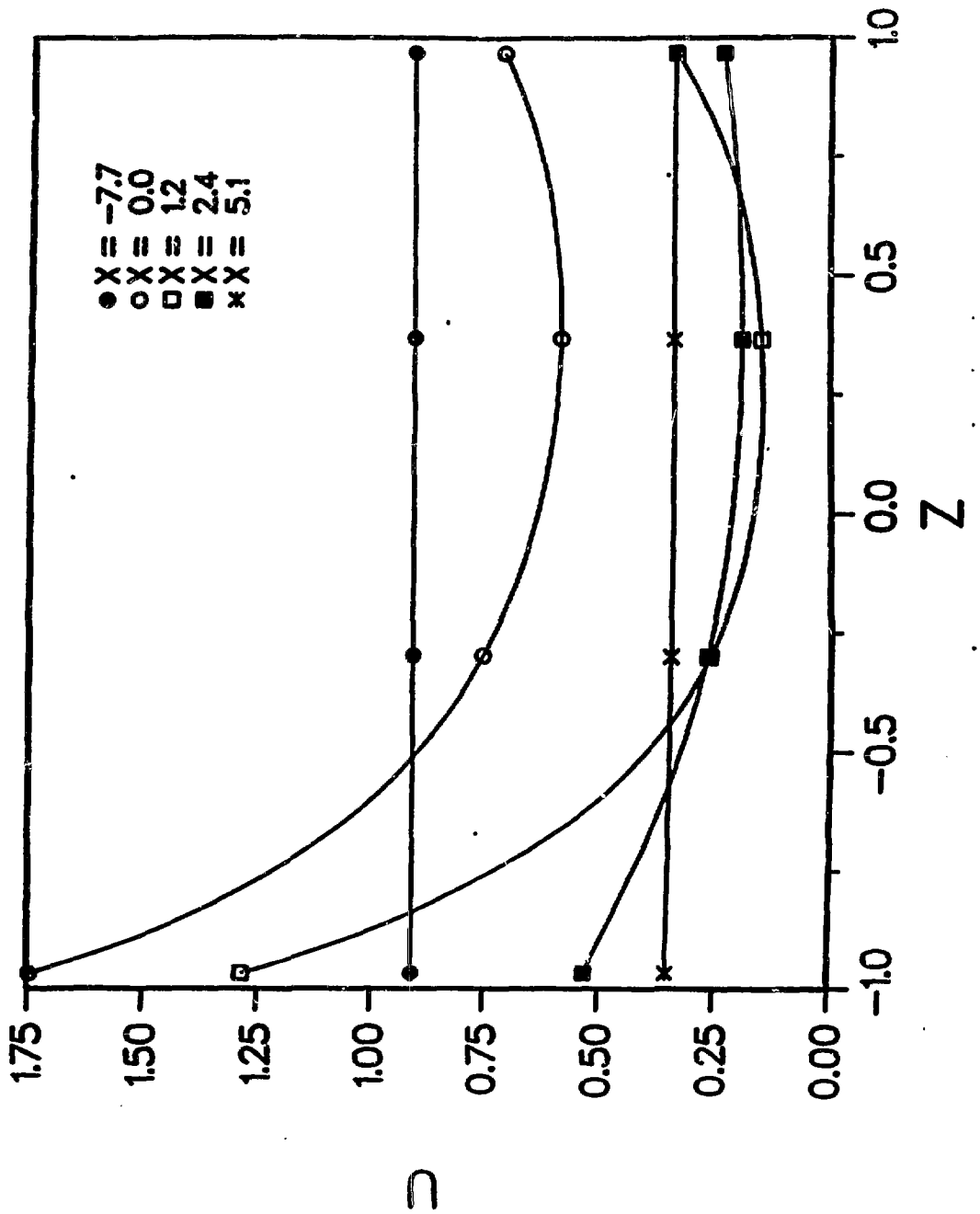

Figure 5 (Thanh Hua, et al.)

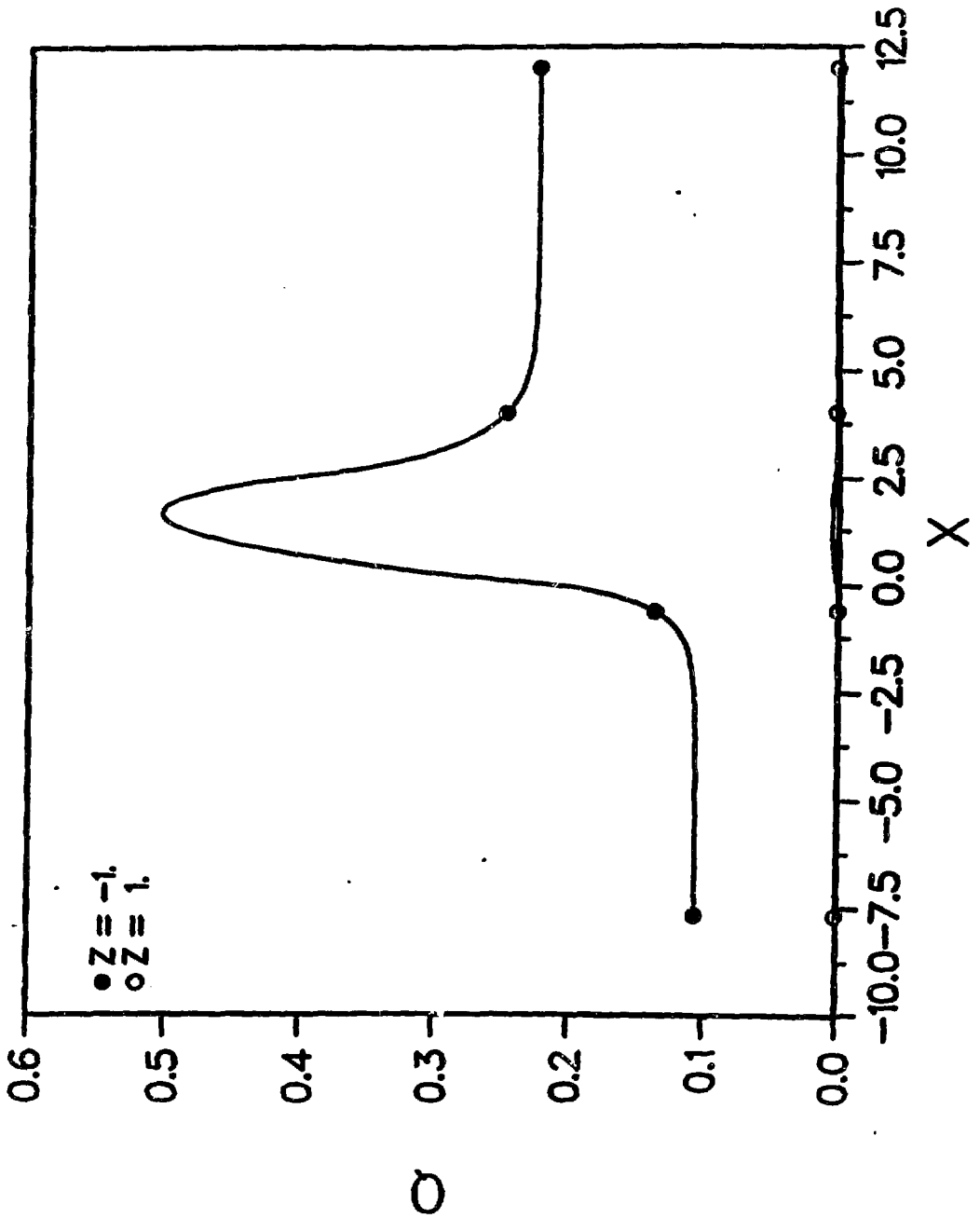

Figure 6 (Thanh Hua, et al.)

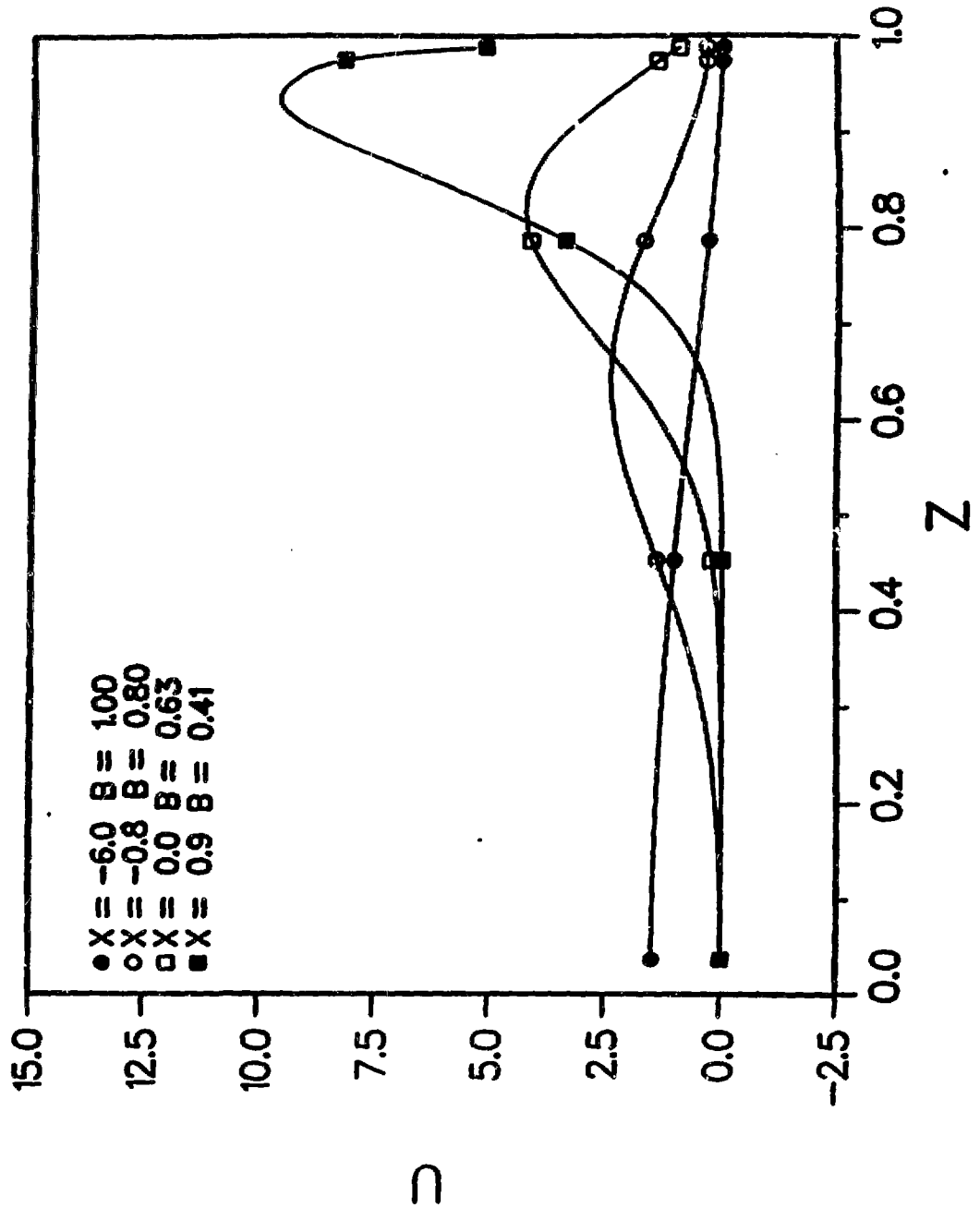

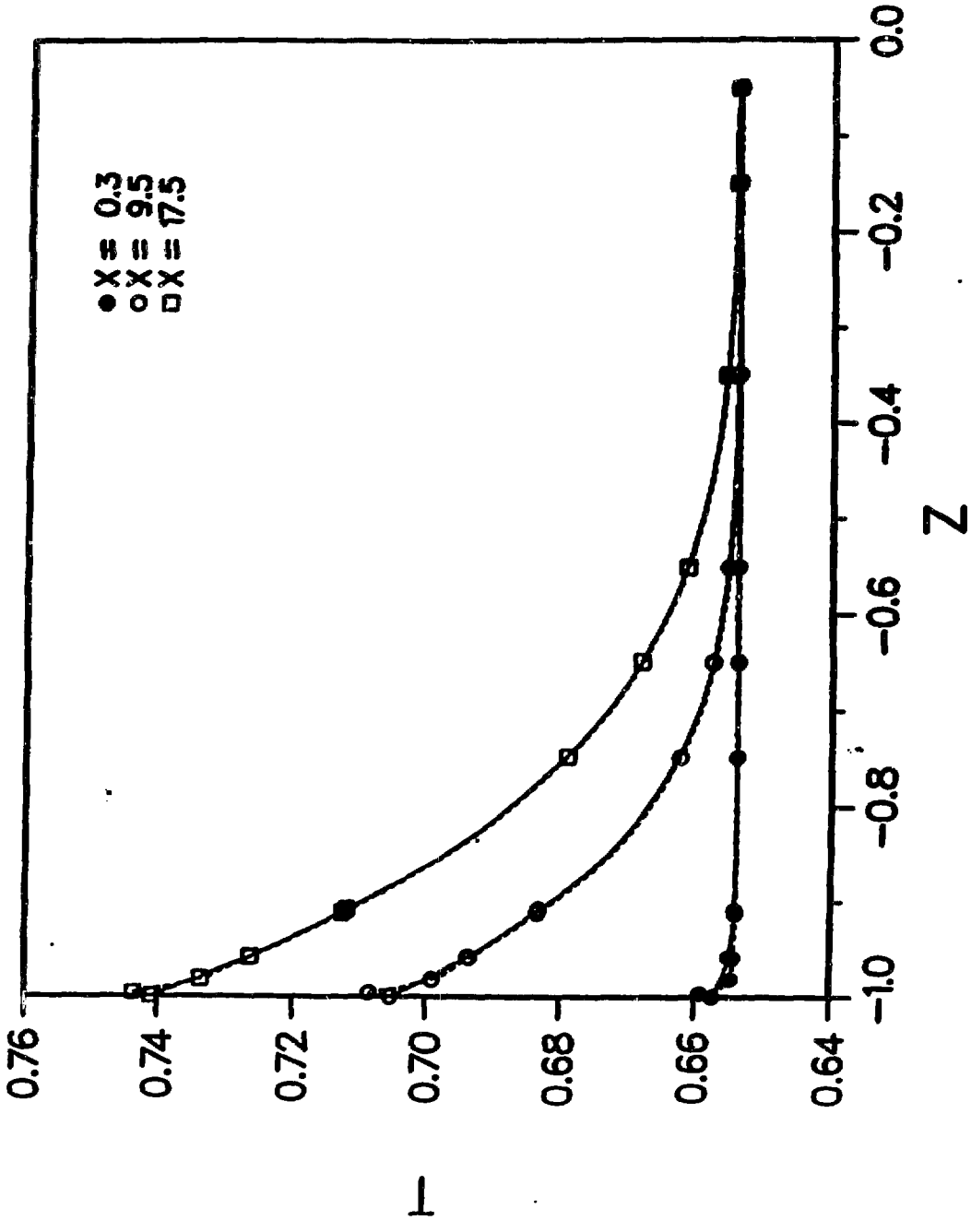
X = 0.3
X = 9.5
X = 17.5
0.0
-0.2
-0.4
-0.6
-0.8
-1.0
Z
0.76
0.74
0.72
0.70
0.68
0.66
0.64
T